Statin or fibrate chronic treatment modifies the proteomic profile of rat skeletal muscle

Giulia Maria Camerino [a], Maria Antonietta Pellegrino [b], Lorenza Brocca [b], Claudio Digennaro [a], Diana Conte Camerino [a], Sabata Pierno [a,1,*], Roberto Bottinelli [b,1]

[a] Department of Pharmacobiology, Section of Pharmacology, Faculty of Pharmacy, University of Bari "Aldo Moro", Via Orabona 4, 70124, Bari, Italy
[b] Department of Physiology and Interuniversity Institute of Myology, University of Pavia, Via Forlanini 6, 27100 Pavia, Italy

ARTICLE INFO

ABSTRACT

Statins and fibrates can cause myopathy. To further understand the causes of the damage we performed a proteome analysis in fast-twitch skeletal muscle of rats chronically treated with different hypolipidemic drugs. The proteomic maps were obtained from extensor digitorum longus (EDL) muscles of rats treated for 2-months with 10 mg/kg atorvastatin, 20 mg/kg fluvastatin, 60 mg/kg fenofibrate and control rats. The proteins differentially expressed were identified by mass spectrometry and further analyzed by immunoblot analysis. We found a significant modification in 40 out of 417 total spots analyzed in atorvastatin treated rats, 15 out of 436 total spots in fluvastatin treated rats and 21 out of 439 total spots in fenofibrate treated rats in comparison to controls. All treatments induced a general tendency to a down-regulation of protein expression; in particular, atorvastatin affected the protein pattern more extensively with respect to the other treatments. Energy production systems, both oxidative and glycolytic enzymes and creatine kinase, were down-regulated following atorvastatin administration, whereas fenofibrate determined mostly alterations in glycolytic enzymes and creatine kinase, oxidative enzymes being relatively spared. Additionally, all treatments resulted in some modifications of proteins involved in cellular defenses against oxidative stress, such as heat shock proteins, and of myofibrillar proteins. These results were confirmed by immunoblot analysis. In conclusions, the proteomic analysis showed that either statin or fibrate administration can modify the expression of proteins essential for skeletal muscle function suggesting potential mechanisms for statin myopathy.

© 2011 Elsevier Inc. All rights reserved.

1. Introduction

Hypocholesterolemic drugs, such as statin and fibrate, are widely prescribed medications effective to reduce blood lipids level. Statins potently inhibit the 3-hydroxymethyl-glutaryl-coenzyme A (HMG-CoA) reductase, the rate-limiting enzyme for the synthesis of mevalonate and therefore cholesterol [1]. Fibrates by acting on the peroxisome proliferator-activated receptor (PPAR)-α, lower serum triglyceride levels and increase high-density lipoprotein (HDL)-cholesterol [2].

Statins and fibrate are generally well tolerated by patients, however they can potentially produce serious adverse effects especially on skeletal muscle. The clinical evidence of statin-associated muscle disorders range from benign myalgia to severe myopathy with elevation of serum creatine kinase (CK) and muscle

weakness. Life-threatening rhabdomyolysis with muscle necrosis and electrolyte alteration, myoglobinuria and renal failure is extremely rare [3–5]. A population-based study describes that the relative risk of myopathy associated with the use of fibrates in monotherapy is 5-fold higher compared with statin [6]. However, the risk of rhabdomyolysis with cerivastatin monotherapy was 10-fold greater than with other statins, and in combination with gemfibrozil, was increased more than 1400-fold [7–9]. Thus, the fear of rare but serious muscle toxicity remains a major impediment to the appropriate use of these drugs considering the ample number of patients worldwide now receiving statins for hypercholesterolemia. In addition statins exhibit anti-inflammatory and antineoplastic pleiotropic effects that may expand their clinical value as well as the need to identify the mechanism of muscle side effects and possibly to find suitable countermeasures [10–12]. Indeed, the precise molecular mechanisms behind statin-associated myopathy have not been fully elucidated, although various hypotheses suggested either the alteration of muscle cell membrane function due to impairment of cholesterol synthesis, the deficits in energy metabolism associated with ubiquinone deficiency [13] or the reduction of

* Corresponding author at: Tel.: +39 080 5442761; fax: +39 080 5442801.
E-mail address: spierno@farmbiol.uniba.it (S. Pierno).
[1] These authors contributed equally to this work as senior authors.

small GTP-binding proteins involved in myocytes preservation [14]. Different studies have shown that statin and fibrate can modify gene and protein expression in skeletal muscle [15]. For instance, an up-regulation of ryanodine receptor, suggestive of intracellular calcium increase, was found in muscle biopsies of statin treated patients showing evident structural damage [16]. Our previous studies have demonstrated that statin and fibrate affect skeletal muscle function also by modifying calcium homeostasis and resting chloride conductance (gCl). Indeed, lipophilic statin increased intracellular calcium via mitochondria and sarcoplasmic reticulum release [17], thereby affecting contractile function. In turn these drugs reduced resting gCl [18,19], a parameter sustained by the ClC-1 chloride channel and modulated by calcium-dependent PKC [20–25]. This parameter is normally high in fast-twitch muscles and is important to guarantee muscle membrane potential and excitability [20–22]. We also found that fenofibrate directly inhibit the ClC-1 chloride channel [20].

To better understand the mechanisms underlying myotoxicity and the diverse effects of statin and fibrate, we applied the proteomic approach to analyze skeletal muscle adaptation to chronic drug treatment. Since statins inhibit many enzymatic reactions downstream of mevalonate production, they may affect a wide range of intracellular functions. Also fenofibrate by acting on peroxisome proliferator-activated receptors (PPARs) has pleiotropic biological effects. In addition, skeletal muscle adaptation is per se very complex because it depends on the activation of genetic programs codifying for proteins belonging to different functional categories [26]. This widens the panorama of potential sites of antilipidemic drug side effects and justifies the difficulties in understanding the mechanisms of myotoxicity. Therefore, since complex modifications of the protein pattern are likely to occur following both statin and fibrate administration, we believe that a global proteomic approach may prove very helpful to clarify the molecular mechanisms underlying myopathy. Thus, the proteomic analysis, by identifying differentially expressed protein following drug administration appears the approach of choice to address the complexity of muscle adaptations and to reveal the underlying mechanisms in statin and fibrate muscle damage. Despite the high resolutive power of the 2DE approach and the large number of proteins whose differential expression could be studied (~450), not all the protein expressed in the muscle could be examined, such as those with an isoelectric point higher than 8–9 and little represented proteins such as membrane proteins. However, this approach has been demonstrated widely useful in a number of recent works [27–30]. Such a proteomic approach is novel in skeletal muscle. The few proteomic studies reported in the literature have regarded other tissues, such as liver and interestingly showed that statin treatment can modify the expression of the cholesterol biosynthesis pathway enzymes as well as of carbohydrate metabolism enzymes, cellular stress proteins and protein involved in calcium homeostasis [31,32]. Statin by inhibiting cholesterol biosynthesis may also affect glutathione peroxidase liver production, whose expression level and catalytic activity were reduced. The consequence of this loss may be an increased sensitivity of the cells to peroxide [33].

Here we report the effects of chronic treatments with fluvastatin, atorvastatin and fenofibrate in rats on the proteomic maps of the extensor digitorum longus (EDL) muscle. Although there are some reports showing that fast-twitch muscles are primarily affected in statin myopathy [34], whereas type I muscle fibers are mainly affected by fibrates [35], we focused the proteomic analysis on the fast-twitch EDL muscle because we previously showed that this muscle is a toxicological target of both statins and fibrates [20]. The results reveal various metabolic pathways involved in the response to antilipidemic drugs, which may concur to myotoxicity.

2. Methods

2.1. Animal care and treatments

The animal study protocol was conducted in accordance with the Italian Guidelines for the use of laboratory animals, which conforms to the European Community Directive published in 1986 (86/609/ EEC). Adult male Wistar rats (Charles River Laboratories, Calco, Italy), weighing 300–350 g, were housed individually in appropriate metabolic cages in an environmentally controlled room and received commercial rodent chow (30 g/day) (Charles River, 4RF21) and water ad libitum. Rats were randomly assigned to 4 experimental groups of 8 animals each: (1) fluvastatin 20 mg/kg/day treated animals (FLUVA), (2) atorvastatin 10 mg/kg/day treated animals (ATO), (3) fenofibrate 60 mg/kg/day treated animals (FENO), (4) control animals (CTRL) treated with the vehicle (0.5% carboxymeth-ylcellulose in aqueous solution) used to dissolve the drugs. Fluvastatin (Lescol, Novartis), atorvastatin (Torvast, Pfizer), and fenofibrate (Lipsin, Caber) were administered orally by using an esophageal cannula, once a day for two months [20]. During the treatment the body weight and vital parameters (health conditions, water and food consumption) were normal in all treated rats. Skeletal muscle performance was evaluated daily by testing in each rat the righting reflex, i.e. the ability of the rat to straighten itself on four legs when turned on the back. The observation of the righting reflex can help to detect severe myotonic-like signs or alteration of muscle function. As previously observed, the righting reflex was normal during the entire treatment period in all the animals. No mortality was observed. At the end of the 2-months treatment rats were sacrificed by cervical dislocation and the extensor digitorum longus (EDL) muscle was carefully dissected from each rat and immediately frozen in liquid nitrogen, then stored at −80 °C until proteomic analysis. The contralateral EDL muscle of all fluvastatin, atorvastatin and fenofibrate treated rats was immediately placed in a appropriate muscle bath chamber to measure the resting chloride conductance (gCl) by the 2-intracellular microelectrode technique [20]. Histological analysis was also performed on four tibialis anterior muscles dissected from randomly selected treated rats of each experimental group as previously described [24].

2.2. Proteome analysis (2-DE)

2.2.1. Sample preparation

The methods of proteome analysis are mostly the same as those previously used [29]. Muscle samples previously stored at −80 °C, were pulverized in a steel mortar with liquid nitrogen to obtain a powder that was immediately resuspended in a lysis buffer [8 M urea, 2 M thiourea, 4% CHAPS, 65 mM DTT, 40 mM Tris base (Healthcare, Germany) and a cocktail of protease inhibitors (Sigma–Aldrich, Italy)]. The samples were vortexed, frozen with liquid nitrogen and thawed at room temperature four times; then the samples were incubated with DNase and RNase for 45 min at 4 °C to separate proteins from nucleic acids and finally spun at $35,000 \times g$ for 30 min. Protein concentration in the dissolved samples was determined with a protein assay kit (2D quant Kit, Healthcare). In order to perform proteome analysis, a sample mix was obtained for each experimental group (CTRL, FLUVA, ATO, FENO). Each sample mix contained an equal protein quantity taken from each muscle sample of CTRL, FLUVA, ATO, FENO.

2.2.2. Two-dimensional electrophoresis

Isoelectrofocusing was carried out using IPGphor system (Ettan IPGphor isoelectric Focusing Sistem – Healthcare). IPG gels strips, pH 3–11 NL (non linear) 13 cm, were rehydrated for 14 h, at 30 V and at 20 °C, in 250 μl of reswelling buffer [(8 M urea, 2 M thiourea, 2% (w/v) CHAPS, 0.1% (v/v) tergitol NP7 (Sigma, Italy),

65 mM DTT, 0.5% (v/v) pharmalyte 3–11NL (Healthcare), tergitol NP7 (Sigma)] containing 100 μg protein sample. Strips were focused at 20,000 V h, at constant temperature of 20 °C and the current was limited to 50 Å per IPG gel strip. After isoelectrofocusing the strips were stored at −80 °C until use or equilibrated immediately for 10–12 min in 5 ml of equilibration buffer [50 mM Tris pH 6.8, 6 M urea, 30% (v/v) glycerol, 2% (w/v) SDS, 3% (w/v) iodoacetamide (Healthcare)]. Then, the immobiline IPG gel strips were applied to 15% SDS–PAGE without a stacking gel. The separation was performed at 80 V for 17 h at room temperature. The 2D gels were fixed for 2 h in fixing solution [(ethanol 40% (v/v) acetic acid 10% (v/v) (VWR International, Italy)], stained with fluorescent staining (FlamingoTM Fluorescent Gel Stain by BIO-RAD, Italy) for 3 h and destained with 0.1% (w/v) Tween 20 (VWR International) solution for 10 min. Triplicate gels of each mix sample were obtained, visualized using a Typhoon laser scanner (Healthcare) and analyzed with Platinum Software (Healthcare). The analysis was performed comparing FLUVA, ATO and FENO with CTRL. For each analysis one gel was chosen as the master gel, and used for the automatic matching of spots in the other 2D gels. Only spots present in all gels used for the analysis were considered. The software provided normalized volume for each spot (representing protein amount). A good reproducibility of the spots among the triplicate gels of each experimental group was found. Plotting the spot volumes for matched spots on a linear scale, in fact, regression analysis yielded correlation coefficients in the range 0.75–0.8. The volumes of each spots in the triplicate gels were averaged and the average volume used for statistical comparison among spots was considered significant if $P < 0.05$. The average volumes of each differentially expressed spot were used to determine the volume ratios reported in the figures and tables.

2.3. Protein identification

2.3.1. Electrophoresis fractionation and in situ digestion

2D gels were loaded with 300 μg of proteins per strip and the electrophoretic was carried out with the same conditions described above. After staining with Colloidal Coomassie (Thermo scientific, UK) spots were excised from the gel and washed in 50 mM ammonium bicarbonate pH 8.0 in 50% acetonitrile (VWR International) to a complete destaining. The gel pieces were re-suspended in 50 mM ammonium bicarbonate pH 8.0 containing 100 ng of trypsin (Sigma–Aldrich) and incubated for 2 h at 4 °C and overnight at 37 °C. The supernatant containing the resulting peptide mixtures was removed and the gel pieces were re-extracted with acetonitrile. The two fractions were then collected and freeze-dried.

2.3.2. MALDI MS analysis

MALDI mass spectra were recorded on an Applied Biosystem (Italy) Voyager DE-PRO mass spectrometer equipped with a reflectron analyzer and used in delayed extraction mode. 1 μl of peptide sample was mixed with an equal volume of α-cyano-4-hydroxycynnamic acid as matrix [10 mg/ml in 0.2% TFA in 70% acetonitrile (VWR International)], applied to the metallic sample plate and air dried. Mass calibration was performed by using the standard mixture provided by the manufacturer. Mass signals were then used for database searching using the MASCOT peptide fingerprinting search program (Matrix Science, Boston, USA) available on the net.

2.3.3. LC–MS–MS analysis

When the identity of the proteins could not be established by peptide mass fingerprinting, the peptide mixtures were further analyzed by LC–MS–MS using the LC/MSD Trap XCT Ultra (Agilent Technologies, Palo Alto, CA) equipped with a 1100 HPLC system and a chip cube (Agilent Technologies). After loading, the peptide mixture [7 μl in 0.5% TFA (VWR International)] was first concentrated and washed (i) at 1 μl/min onto a C18 reverse-phase pre-column (Waters, USA) or (ii) at 4 μl/min in 40 nl enrichment column (Agilent Technologies chip), with 0.1% formic acid (VWR International) as the eluent. The sample was then fractionated on a C18 reverse-phase capillary column (75 mm × 20 cm in the Waters system, 75 mm × 43 mm in the Agilent Technologies chip) at a flow rate of 200 nl/min, with a linear gradient of eluent B [0.1% formic acid in acetonitrile (VWR International)] in A (0.1% formic acid) (VWR International) from 5% to 60% in 50 min. Elution was monitored on the mass spectrometers without any splitting device. Peptide analysis was performed using data-dependent acquisition of one MS scan (m/z range from 400 to 2000 Da/e) followed by MS/MS scans of the three most abundant ions in each MS scan. Dynamic exclusion was used to acquire a more complete survey of the peptides by automatic recognition and temporary exclusion (2 min) of ions from which definitive mass spectral data had previously been acquired. Moreover a permanent exclusion list of the most frequent peptide contaminants (keratins and trypsin peptides) was included in the acquisition method in order to focus the analyses on significant data.

2.4. Immunoblot analysis

The validation of expression changes of the proteins as judged by 2-DE analysis was carried out by standard 1-D immunoblotting. About 30 μg of muscle samples prepared and used for 2D electrophoresis were loaded on 15% polyacrylamide SDS–PAGE gels. The proteins were electrotransferred from gels to nitrocellulose membranes (4.5 μm pore size, Healthcare product, Germany) and the Western blot analysis was performed. Nitrocellulose membranes were blocked in 5% milk in TBS (Tris 0.02 M, NaCl 0.05 M pH 7.4–7.6) for 1 h and then incubated in primary antibody (diluted in 5% milk) at 4 °C overnight. The membranes were probed with antibody specific to ATP synthase (rabbit-anti ATP synthase, 1:2500, from Abcam, Italy), isocitrate dehydrogenase (rabbit-anti Isocitrate Dehydr, 1:500, from Abcam), Pyruvate kinase (rabbit polyclonal anti pyruvate kinase, 1:1000, from Abcam), Glyceraldehyde 3-P dehydrogenase (rabbit polyclonal anti GAPDH, 1:1000, from Abcam), Triosephosphate isomerase (goat polyclonal anti Triosephosphate isomerase 1:1000, from Biocompare, Italy), Creatine Kinase M (rabbit-anti CK M, 1:1000, from Abcam) Hsp1 (mouse-anti Hsp27, 1:1000, from Abcam). After several rinses in TTBS (0.1% Tween-20 in TBS, VWR International), the membranes were incubated in HRP-conjugated secondary antibody (diluted in 5% milk), rabbit-anti-mouse (1:800, from Dako, USA), rabbit-anti-goat (1:5000, from Abcam) or goat-anti-rabbit (1:5000, from Millipore, Italy) for 1 h at room temperature. The protein bands were visualized by an enhanced chemiluminescence method in which luminol was excited by peroxidase in presence of H_2O_2 (ECL Plus, Healthcare product). The content of single protein investigated was assessed by determining the brightness-area product (BAP) of the protein bands.

2.5. Analysis of MHC isoforms content

About 6 μg of each muscle sample were dissolved in lysis buffer containing 8 M, 2M thiourea, 4% CHAPS, 65 mM DTT and 40 mM Tris base [36]. The lysates were applied onto 8% poyacrylamide SDS–PAGE gels prepares according to the method described by Talmadge and Roy [37]. Electrophoresis was run for 2 h at 200 V and then for 24 h at 250 V. The gels were stained with Coomassie blue staining. In the region of MHC isoforms, four bands were separated that corresponded, in order of migration from the fastest to the slowest, to MHC-1 (or slow), MHC-2B, MHC-2X and MHC-2A (or fast). Densitometric analysis of these isoforms were performed

to establish the relative proportion of the MHC isoforms identified in the sample [38].

2.6. Creatine kinase determination

Blood was collected by cardiac puncture, soon after animal death, in ethylenediaminetetraacetic acid (EDTA, Sigma) rinsed centrifuge tubes. The blood was centrifuged at $600 \times g$ for 10 min at 15 °C and the plasma was separated and stored at −20 °C until assay. Creatine kinase determination was performed by standard spectrophotometric analysis by using diagnostic kit (Sigma–Aldrich, Milan, Italy) within 7 days from plasma preparation [24].

2.7. Statistical analysis

Data were expressed as mean ± S.E.M. Statistical significance of the differences between means was assessed by Student's t-test or by one-way ANOVA followed by Student–Newman–Keuls test (for data in Fig. 3). A probability of less than 5% was considered significant ($P < 0.05$).

3. Results

3.1. Analysis of skeletal muscle proteomic map

Proteomic maps of EDL muscles, for each animal of each group (control rats, statin and fibrate treated rats), were obtained using 2D gel electrophoresis. The comparison between 2D maps of treated and control rats enabled us to identify the differentially expressed proteins which were thereafter identified by MALDI. Such proteins are indicated by circles and numbers in the control maps of EDL as reported in Fig. 1. The full set of information regarding the differentially expressed proteins is reported in Table 1. The differentially expressed proteins were grouped on the basis of their functional role in the following categories: energy production system (oxidative metabolism, glycolytic metabolism and creatine kinase), myofibrillar proteins, detoxification systems and other proteins (Fig. 2A–C). The proteomic map of control rat showed about 450 spots. In EDL of atorvastatin treated rat about 417 spots were found. The comparison between the protein spots common to atorvastatin and CTRL maps showed that the 9.6% (40 spot) of spots

Fig. 1. Typical 2D pattern gel image of proteins extract of control EDL muscles. The protein spots found to be differentially expressed in EDL muscles of control vs. EDL muscles of treated rat (with fluvastatin, atorvastatin or fenofibrate) are circled and numbered. The numbers enable to identify the spots using Fig. 3 and Table 1.

were significantly different. Of the 40 spots (15 identified by mass spectra analysis) 2.5% ($n = 1$) were up-regulated and 97.5% ($n = 39$) were down-regulated. In EDL of fluvastatin treated rat about 436 spots were found. Compared to control only the 3.4% (15 spot) of the spots showed significant differences in protein expression. Of the 15 spots (6 identified by mass spectra analysis) 12.5% ($n = 2$) were up-regulated and 86.6% ($n = 13$) were down-regulated. In EDL of fenofibrate treated rat about 439 spots were found. In fenofibrate maps the percent of significantly different spots was 5% (21 spots), compared to CTRL. Of the 21 spots (12 identified by mass spectra analysis) 14% ($n = 3$) were up-regulated and 86% ($n = 18$) down-regulated. Several of the differentially expressed proteins reported in Fig. 1 and Table 1, were found in multiple spot localizations (see, for example, glyceraldehyde 3-phosphate dehydrogenase in fenofibrate map and creatine kinase and pyruvate kinase in atorvastatin map) and therefore appear more than once in Fig. 2. The presence of multiple spots of a protein is frequent in 2D gels and is due to the existence of isoforms or to post-translational modifications of proteins. Different isoforms of the same protein might differ both for molecular weight and isoelectric point, or different molecular weight. Mass spectrometry was not able to identify all isoforms of some proteins or the nature of their post-translational modifications. To make sure that the change in expression of the identified spot or spots of a given protein was representative of the global change of that protein, the expression of the most relevant proteins was confirmed by western blot on one dimensional gels. In the latter gels, in fact, all the spots of a protein which are separated in 2D gels migrate in a single band.

3.2. Energy production system

The larger group of differently expressed proteins was involved in the three energy production systems: oxidative metabolism, glycolitic metabolism and creatine kinase. EDL of atorvastatin treated rats showed a down regulation of four proteins involved in oxidative metabolism [isocytrate dehydrogenase 3 (−5.49 ratio), NADH dehydrogenase 1 (−1.98 ratio), oxoglutarate dehydrogenase (−1.9 ratio), ATP synthase (β subunit) (−6.43 ratio)]. The glyceraldehyde 3 phosphate dehydrogenase, enolase 3 and three isoforms of pyruvate kinase (spot number 8, 9 and 10), that are involved in glycolytic metabolism, were also down-regulated (−3.30, −3.17, −3.01, −1.377 and −2.39 ratio, respectively) (Table 1). EDL of fluvastatin treated animals did not show significant alterations of proteins involved in energy production systems, except for 2 isoforms of β enolase 3 (protein of glycolitic system) that was less expressed if compared to control (−2.20 and −1.73 ratio in spot number 1 and 2, respectively) (Table 1). In contrast, the fenofibrate maps showed small alterations of the enzymes involved in oxidative metabolisms and a marked down-regulation of proteins involved in the glycolytic metabolism. The ATP synthase, in particular the mitochondrial β subunit (−2.29 ratio), which belongs to the oxidative system, was down-regulated. Triosephosphate isomerase, β enolase 3, and 2 isoforms of glyceraldehde 3 phosphate dehydrogenase (spot number 22 and 23), which belongs to glycolytic systems, were down-regulated (−1.91; −4.09; −2.35 and −6.08 ratio, respectively). On the contrary the pyruvate kinase was up-regulated (2.17 ratio) (Table 1). EDL of fenofibrate and atorvastatin treated rats showed a significant down-regulation of creatine kinase [−1.62 ratio for fenofibrate map (spot number 16) and −2.17; −2.90 ratio for atorvastatin map (spot number 16 and 17)] compared to CTRL.

3.3. Myofibrillar proteins

All treatments resulted in some alteration in myofibrillar protein expression. The troponin T type IVc was down-regulated in
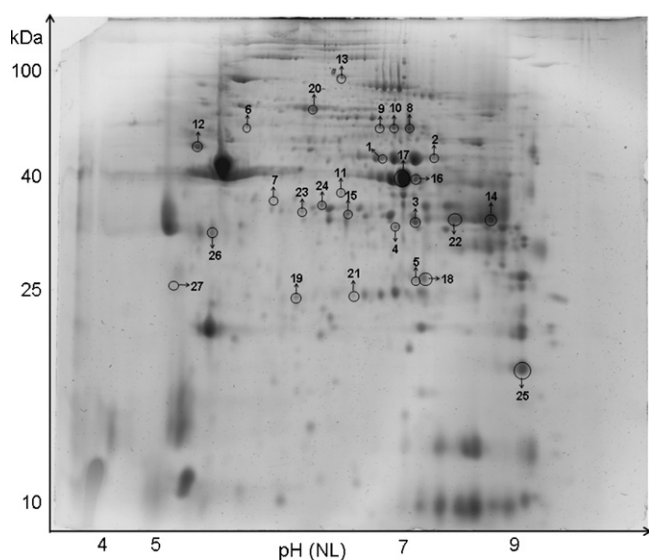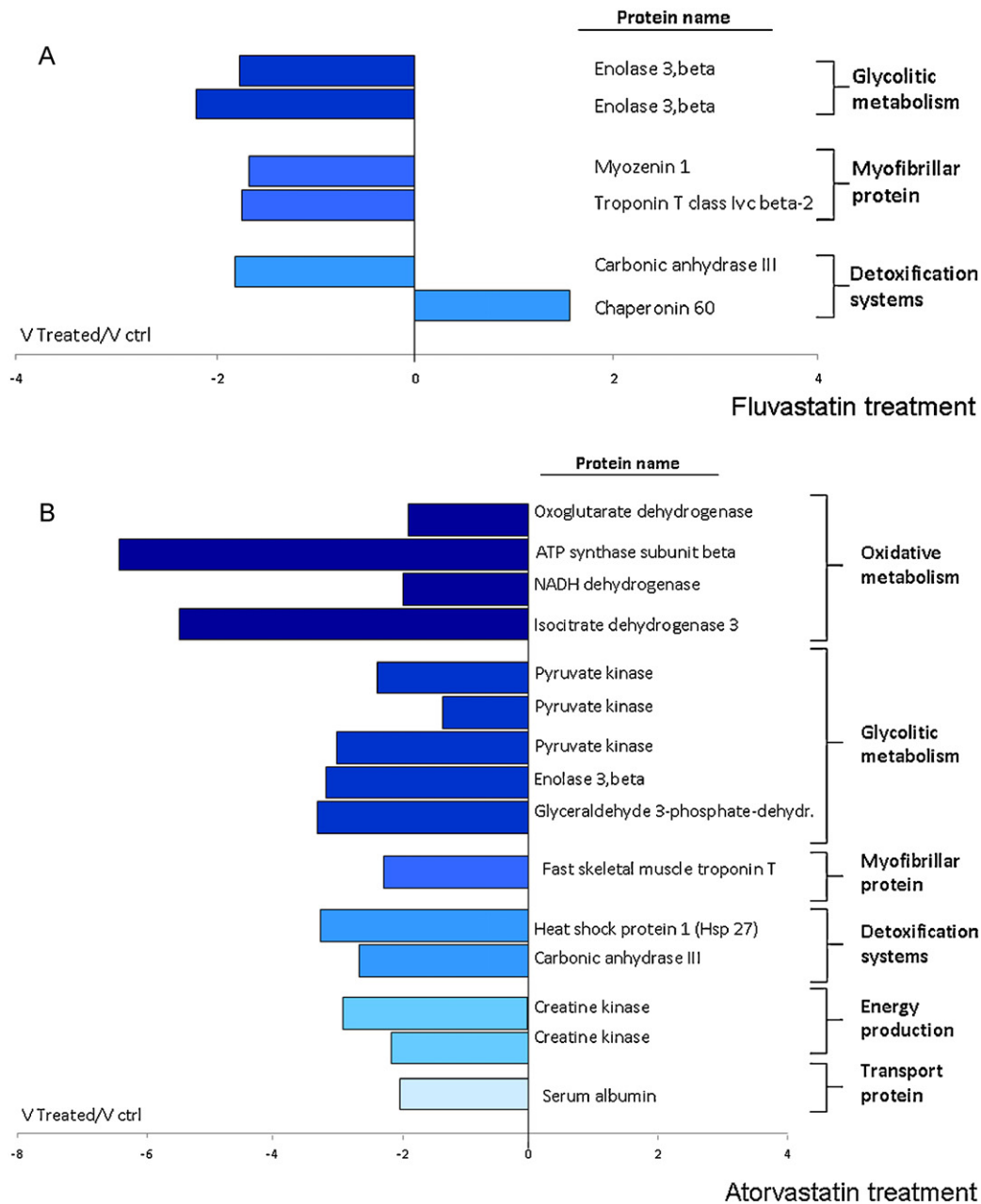
Fig. 2. Histogram of volume ratios of differentially expressed proteins of EDL muscles of rat treated with fluvastatin (panel A) atorvastatin (panel B) and fenofibrate (panel C) in comparison to control. As reported on the right, proteins were grouped on the basis of functional role in: energy production proteins (oxidative metabolism, glycolitic metabolism and creatine kinase) myofibrillar proteins and detoxification proteins and other proteins. The numbers on the X-axis indicate the ratio between the average volume of a given protein expressed in EDL muscles of rats treated and the average volume of the same protein in control EDL muscles. Positive numbers (on the right) indicate up-regulation of proteins in the treated rats, whereas negative numbers (on the left) indicate down-regulation.

muscles treated with fenofibrate (−1.84 ratio), and fluvastatin (−1.71). The troponin T fast and α-2 actin were down-regulated following fenofibrate treatment (−3.21 and −1.95, respectively). In fluvastatin treated muscles myozenin 1 was down regulated (−1.64 ratio). The troponin T fast was down-regulated following atorvastatin treatment (−2.29 ratio) (Table 1). The adaptations in myofibrillar protein isoforms, consistent with the lack of variation in MHC isoform composition, did not show any trend of a shift in muscle phenotype (Fig. 3).

3.4. Detoxification system

Statin and fibrate had an impact on detoxification and on antioxidant proteins. The heat shock protein 1 was, indeed, down-regulated after treatment with atorvastatin and fenofibrate (−3.26 and −1.85 ratio, respectively). The carbonic anhydrase III was under-expressed after fluvastatin and atorvastatin treatments (−1.78 ratio and −2.66, respectively). The map of EDL muscle treated with fluvastatin showed a overexpression of chaperonin 60 (1.57 ratio) (Table 1).

3.5. Other proteins

The atorvastatin map showed a down regulation of serum albumin, a known plasma protein carrier (−2.03 ratio). The muscles treated with fenofibrate showed an important reduction of the expression of MSF mitochondrial factor, an important stimulation factor (−6.62 ratio) (Table 1).
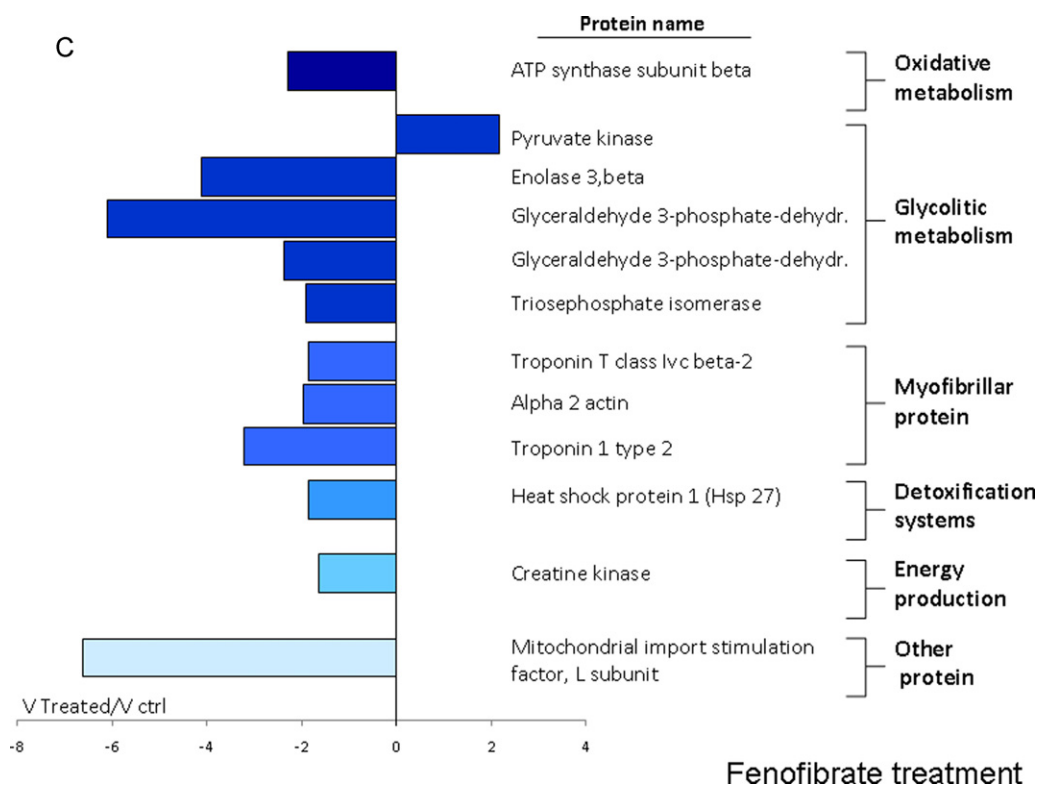
Fig. 2. (Continued).

3.6. Immunoblot analysis

To validate the results of 2-DE analysis comparative immuno-blotting of some of most relevant changed proteins was carried out. Comparative analysis of immunoreactive bands of ATP synthase, isocitrate dehydrogenase, pyruvate kinase, glyceraldehyde 3-P dehydrogenase, triosephosphate isomerase, creatine kinase, Hsp1 in the different treatments, confirmed, at the level of the whole protein, the change in expression of the protein spot/s revealed by 2D gels (Fig. 4).

3.7. Biological and functional indexes of skeletal muscle toxicity

To verify the possible impairment of skeletal muscle due to statin or fibrate chronic treatment we examined the release of creatine kinase (CK) from myocytes into the bloodstream. Thus, we measured CK level in plasma of all treated rats and compared those with control. Fluvastatin at the higher dose (20 mg/kg) significantly increased (about 3-fold) the plasma CK content, while no significant effect was found in the rats treated with the lower dose (Table 2). Also atorvastatin and fenofibrate, at the doses tested, significantly increased plasma CK level about 3-fold or 2-fold, respectively, with respect to control (Table 2). The histopathological analysis of tibialis muscle did not show any modification of muscle section (data not shown), as previously described [24]. Moreover, as already demonstrated [24], in all the rats treated with fluvastatin, atorvastatin or fenofibrate the resting gCl was significantly reduced (no more than 30%) with respect to the control value (data not shown).

4. Discussion

Taking advantage of the high resolving power and of the very large number of proteins sampled by the proteomic analysis, this novel study demonstrates that statins and fibrate administration induce complex modifications of the protein pattern of skeletal muscle, suggesting an effect on a wide range of biological functions (Supplementary Fig. S1). In parallel, other studies performed by using combined genomic and lipidomic analysis showed changes in muscle metabolism (dysregulation of calcium binding proteins and phospholipase C pathway, defective mitochondrial metabolism and activation of pro-apoptosis pathway, dysregulation of cell membrane lipids) contributing to muscle toxicity [39]. Our results showed a down-regulation of several muscle proteins and this effect was confirmed by the western blot experiments. Proteins involved in energy production and in detoxification systems were the major sets of differentially expressed proteins and their changes could lead to the generation of myopathy. Atorvastatin induced a modification of a larger number of proteins than fluvastatin and fenofibrate. The reason may be related to the different chemical structure or the longer half-life of atorvastatin in comparison to the other drugs tested.

4.1. Myofibrillar proteins

Muscle plasticity is a particular feature of skeletal muscle by which different stimuli (disuse, drugs, etc.) can induce phenotype transition. For instance, hindlimb unloading of rodents, a model of muscle disuse, induce a slow-to-fast transition of postural muscles, i.e. increased expression of fast isoforms of myosin heavy chain (MHC) and increase of resting gCl in soleus muscle [40]. A coordinated expression existed among MHC isoforms, metabolic enzymes and isoforms of other myofibrillar and non-myofibrillar proteins [41–43]. Therefore, in most myopathic conditions the change in expression of many proteins can be related to the activation of a single gene expression program aimed to coordinately adapt muscle contractile machinery, energy production and cytoskeleton. To test if statin or fibrate can produce phenotype transition, we measured MHC isoform distribution in the EDL muscle. The lack of any change in MHC isoform distribution indicates that the large changes in the protein pattern due to statin and fibrate administration occur independently from

Table 1
Proteins differentially expressed and related changes in EDL muscles of rats following treatment with statins or fenofibrate.

Spot no.	Protein name	Accession num.	Fold change	MOWSE	P value	Th Pi	Th MW	Pathway
Fluvastatin								
1	Enolase 3	gi126723393	−2.20323	90	0.0491	7.08	47,326	Glycolitic metabolism
2	Enolase 3	gi126723393	−1.7359	412	0.039	7.08	47,326	Glycolitic metabolism
3	Troponin T class IVc beta-2	gi207403	−1.711174	383	0.0258	9.36	28,595	Myofibrillar systems
4	Myozenin 1	gi157819165	−1.64106	216	0.049	8.57	31,379	Myofibrillar systems
5	Carbonic anhydrase III	gi31377484	−1.78059	497	0.0203	6.89	29,698	Detoxification systems
6	Chaperonin 60	gi1778213	1.57865	389	0.0492	5.78	61,029	Detoxification systems
Atorvastatin								
7	Isocitrate dehydrogenase 3 (NAD+) alpha precursor	gi16758446	−5.49956	221	0.0014	6.47	40,044	Oxidative metabolism
8	Pyruvate kinase	gi16757994	−3.01587	870	0.0023	6.63	584	Glycolitic metabolism
9	Pyruvate kinase	gi16757994	−1.37775	976	0.033	6.63	58,294	Glycolitic metabolism
10	Pyruvate kinase	gi16757994	−2.39449	1008	0.0082	6.63	58,294	Glycolitic metabolism
11	NADH dehydrogenase (ubiquinone) 1 alpha subcomplex 10-like	gi32996721	−1.98637	309	0.0172	7.14	40,804	Oxidative metabolism
12	ATP synthase subunit beta. mitochondrial	gi1374715	−6.43293	510	0.0012	4.95	51,710	Oxidative metabolism
13	Oxoglutarate (alpha-ketoglutarate) dehydrogenase (lipoamide) precursor	gi62945278	−1.90863	333	0.0298	6.3	117,419	Oxidative metabolism
14	Glyceraldehyde 3-phosphate-dehydrogenase	gi56188	−3.3096	316	0.0076	8.43	36,098	Glycolitic metabolism
2	Enolase 3	gi126723393	−3.179	412	0.047	7.08	47,326	Glycolitic metabolism
15	Fast skeletal muscle troponin T	gi136385	−2.29568	267	0.019	6.19	30,732	Myofibrillar systems
16	Creatine kinase	gi6978661	−2.17813	530	0.0043	6.58	43,220	Energy production system
17	Creatine kinase	gi6978661	−2.90683	480	0.019	6.58	43,220	Energy production system
18	Carbonic anhydrase III	gi31377484	−2.66095	375	0.0032	6.89	29,698	Detoxification system
19	Heat shock protein 1	gi94400790	−3.26578	265	0.0024	6.12	24,860	Detoxification system
20	Serum albumin	gi124028612	−2.03454	162	0.0361	6.09	70,682	Transport protein
Fenofibrate								
21	Triosephosphate isomerase	gi38512111	−1.91293	298	0.0031	7.06	26,717	Glycolitic metabolism
22	Glyceraldehyde 3-phosphate-dehydrogenase	gi56188	−2.35928	171	0.001	8.43	36,098	Glycolitic metabolism
23	Glyceraldehyde 3-phosphate-dehydrogenase	gi56188	−6.08448	183	0.0049	8.43	36,098	Glycolitic metabolism
24	Enolase 3	gi126723393	−4.09962	601	0.0002	7.08	47,326	Glycolitic metabolism
12	ATP synthase subunit beta, mitochondrial	gi1374715	−2.29476	234	0.0001	4.95	51,710	Oxidative metabolism
10	Pyruvate kinase	gi16757994	2.171749	870	0.0008	6.63	58,294	Glycolitic metabolism
25	Troponin I, fast skeletal muscle	gi8394466	−3.21101	134	0.001	8.86	21,486	Myofibrillar system
26	Alpha 2 actin	gi4501883	−1.95422	250	0.0093	5.24	41,774	Myofibrillar system
3	Troponin T class IVc beta-2	gi207403	−1.84166	383	0.042	9.36	28,595	Myofibrillar system
16	Creatine kinase	gi6978661	−1.62055	656	0.035	6.58	43,220	Energy production system
19	Heat shock protein 1	gi94400790	−1.85726	265	0.036	6.12	24,860	Detoxification system
27	Mitochondrial import stimulation factor L subunit	gi61216932	−6.62572	150	0.0285	4.63	29,173	Other proteins

In the table are showed: the spot number corresponding to the number reported in Fig. 2; the name of proteins; the accession number corresponding to NCBI; the related fold changes of proteins are expressed in average ratio of change relative to the control (V Treated/V ctrl); MOWSE score; P value; the experimental Pi; the experimental MW; the biochemical pathway group membership.

such major gene expression program, suggesting more a toxic action than a functional adaptation of the treatments. This observation especially applies to changes in energy production systems which are generally under the same control as MHCs, but deeply change following statin and fibrate treatments. The observed changes in myofibrillar and cytoskeleton proteins

Fig. 3. Myosin heavy chain (MHC) isoform distribution in EDL muscles of rat control (CTRL) and treated with fluvastatin (FLUVA), atorvastatin (ATO) and fenofibrate (FENO). MHC isoform distribution was determined by SDS–PAGE separation and subsequent densitometric analysis of MHC bands. The height of each vertical bar represents the mean values (±S.E.M).

(Troponin type IVc, Troponin T fast, α-2 actin, myozenin) do not have a straightforward interpretation in the frame of known structural or functional alteration of statin myopathy, but confirm that statins and fibrates can act directly on proteins independently from muscle phenotype.

4.2. Muscle cellular energy metabolism

Both statins and fenofibrate induced critical alterations of energy metabolism enzymes: atorvastatin down-regulated different oxidative and glycolytic enzymes, whereas fenofibrate mainly affected glycolytic enzymes. This latter finding can be a consequence of the inhibition of the specific targets of the two drugs. Otherwise, the prevalent effect of atorvastatin on the oxidative metabolism pathway can be related to the already described statin-mediated mitochondrial involvement [17,19,39]. Yet, since fenofibrate have no effects on calcium released by mitochondria [17], likely slight effect on the oxidative metabolism were observed here.

4.2.1. Oxidative metabolism

Two biochemical pathways part of the oxidative metabolism, such as the Krebs cycle and the mitochondrial respiratory chain, are affected by atorvastatin treatment. Indeed two enzymes that participate to Krebs cycle, such as isocitrate dehydrogenase (which
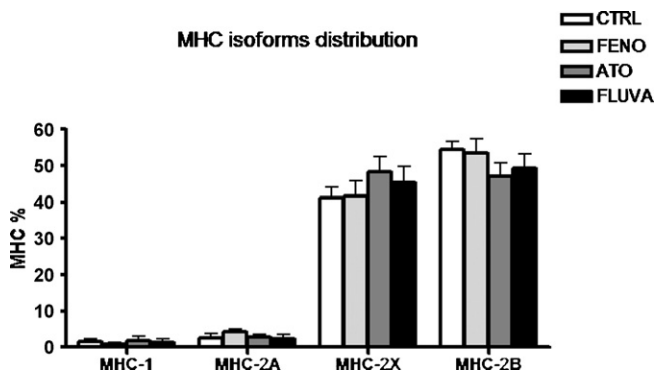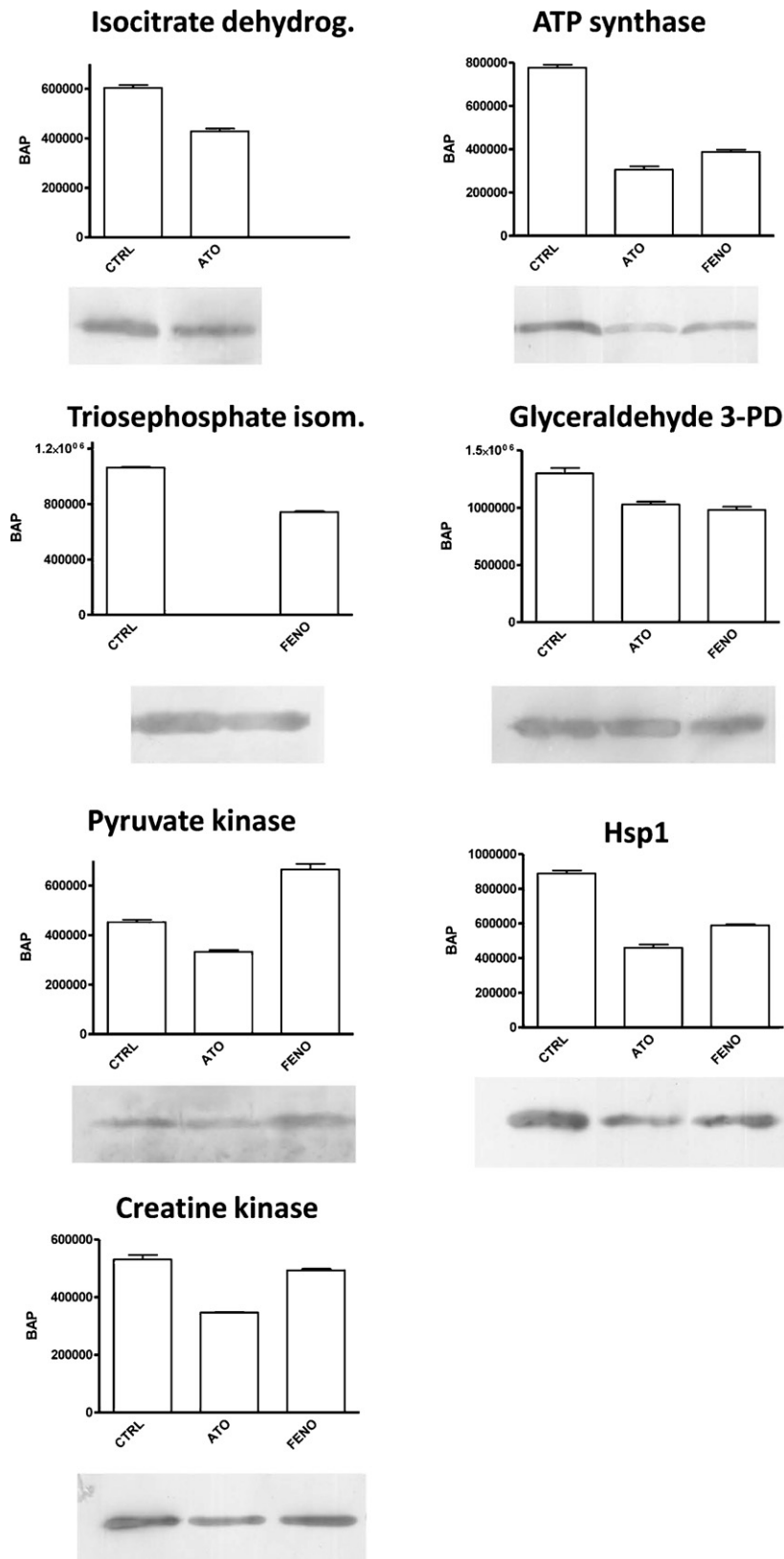
Fig. 4. Confirmation of the proteomic data by Western blot analysis. The figure shows immunoreactive bands of ATP synthase, isocitrate dehydrogenase, pyruvate kinase, glyceraldehyde 3-P dehydrogenase, triosephosphate isomerase, creatine kinase, Hsp1 and their quantification by the levels of brightness area product (BAP) in control (CTRL) mice and mice treated with atorvastatin (ATO) and fenofibrate (FENO).

converts isocitrate in oxoglutarate) and the oxoglutarate dehydro-genase (which converts ketoglutarate in succinyl CoA) are down-regulated. Both enzymes are NAD dependent and their down-regulation can affect NADH production, then blocking the pathway

and ATP production during mitochondrial electron transport. In consequence the acetyl CoA may accumulate in the mitochondria due to the block of the Krebs cycle and in the cytosol, because it is the first substrate of cholesterol synthesis that is inhibited by the

Table 2
Effects of two months chronic treatment with statins or fenofibrate on rat plasma creatine kinase.

Treatment	N	CK (U/l)	Bonferroni t-test vs. control
Control	8	863 ± 210	
Fluvastatin 5 mg/kg	8	1011 ± 199	ns
Fluvastatin 20 mg/kg	8	2358 ± 250	$P < 0.001$
Atorvastatin 10 mg/kg	8	2561 ± 244	$P < 0.001$
Fenofibrate 60 mg/kg	8	1844 ± 217	$P < 0.005$

The values of creatine kinase (CK) measured in plasma of control and treated rats are expressed as mean $\pm$ S.E.M. from the number (N) of animals as indicated. Data showed significant differences by ANOVA test ($F = 11.7$, df $= 4/35$, $P < 0.001$) followed by Bonferroni t-test.

statin. Increase of acetyl-CoA is known to inhibit the pyruvate kinase (PK) and to slow the glycolysis. The enzymes NADH dehydrogenase (ubiquinone) and ATP synthase, involved in the mitochondrial respiratory chain, were also altered by atorvastatin treatment. As already suggested, ubiquinone reduction may be responsible for statin induced muscle damage [19]. For instance it has been shown that simvastatin was able to reduce ubiquinone level and mitochondrial function in human skeletal muscle [44]. Although controversial data have been reported [45,46], it has proposed that muscle cell treatment with ubiquinone can restore statin-induced muscle damage [47]. Thus the observation that NADH dehydrogenase was down-regulated in the proteomic map of atorvastatin treated skeletal muscles strongly support the hypothesis of mitochondrial involvement [17]. Another novelty of the present study is the down-regulation and defect of the catalytic subunit of ATP synthase due to atorvastatin treatment, which may lead to ATP level reduction and consequent metabolic stress. Accordingly, a reduction of intracellular ATP content has been already described in human myocytes due to atorvastatin [48]. Here we also find a minor involvement of ATP synthase in fenofibrate treated rats supporting the lesser participation of mitochondria in skeletal muscle damage induced by fenofibrate [17].

4.2.2. Glycolytic metabolism

Both fenofibrate and statins resulted in a down-regulation of glycolytic enzymes expression. The beta enolase was down-regulated in all treatments, the PK was down-regulated in rats treated with atorvastatin and glyceraldehyde-3-phosphate dehydrogenase was down-regulated following atorvastatin and fenofibrate treatments. Another glycolytic enzyme, such as the triose-phosphate isomerase, essential for energy production, was down-regulated after fenofibrate treatment. The slow-down of glycolysis can be justified by the increased ß-oxidation pharmacologically induced by PPAR mediated fibrate or statin activation [49]. The down-regulation of glycolytic enzymes is a symptom of energy production failure, and can contribute to muscle damage. Interestingly a general impairment of energy metabolism have been observed in conditions of muscle atrophy [29], which may develop also during statin myopathy [50]. Moreover, it has been shown that hereditary muscle glycogenoses in humans are characterized by defective glycolytic enzymes, including beta enolase, and leads to different degree of myopathy, ranging from cramps to myoglobinuria [51,52]. The PK is a key enzyme in the glycolytic pathway, being responsible for the synthesis of pyruvate and ATP formation; it is allosterically inhibited by the increase in acetyl CoA, which in this condition may be induced by the block of cholesterol pathway in the cytosol. Interestingly, in fenofibrate treated rats the PK is up-regulated, although many enzymes of the glycolytic pathway are down-regulated, possibly because the oxidative and cholesterol pathway are not affected.

4.3. Energy production system: creatine kinase

Muscle damage induced by statin and fibrate is associated with an increase of creatine kinase (CK) level in the plasma. For instance, other authors found a plasma CK increase in correlation with histological damage due to cerivastatin induced skeletal muscle damage [53]. Here we found an increase of plasma CK in all treated rats not followed by histological modification likely because the drugs we used were less toxic. Moreover, we found a decrease of CK expression in muscle treated with atorvastatin and fenofibrate. Since phosphocreatine, produced by CK, is an energy reservoir for different tissues and especially for skeletal muscle, the decrease in CK, together with the observed down-regulation of oxidative and glycolitic enzymes, suggest a general impairment of energy metabolism, which in turn could decrease protein synthesis, an ATP-requiring process. Interestingly, it has been shown that in transgenic mice lacking either the cytoplasmic or mitochondrial CK, muscle atrophy and damage occur [54]. Surprisingly, no modification of CK expression was found in fluvastatin treated rats, in accord with the minor impact of this drug of the whole proteomic pattern.

4.4. Detoxification systems

Statin administration and, to some extent, fibrate administration down-regulated detoxification systems: heat shock protein 1, which protects cells against free radicals produced by stress stimuli, as well as carbonic anhydrase that protects cells against oxidative damage by binding free radicals [55,56]. An effect of statin on HSPs expression has been previously observed in other tissues, such as human placental cells line [57] and rat retina during ischemia [58]. Together with the decrease of muscle plasmalogens, a sub-class of ether phospholipids involved in protection against oxidative damage [39], these effects suggest an accentuated sensitivity of statin-treated muscles to oxidative stress. Oxidative stress has been pinpointed as a likely trigger of many conditions of muscle wasting [59,60].

4.5. Other proteins

Although our previous studies have demonstrated no modification of mitochondrial activity in fibrate-induced myopathy [17], here we found a down-regulation of the mitochondrial stimulation factor (MSF) important for the synthesis and folding of mitochondrial ATP-dependent protein precursor [61], likely suggesting an alteration in the number of these organelles in fenofibrate-treated muscles. We also found a down-regulation of serum albumin in atorvastatin-treated muscles likely supporting the lack of its scavenger activity in the muscle. At this regard the effects of statin on albumin expression is controversial: simvastatin has been found to increase albumin synthesis contributing to reduce cardiovascular risk since it transport plasma lipids [62].

5. Concluding remarks

By using a proteomic approach we identified new toxicological markers of myopathy induced by hypolipidemic drugs (Supplementary Fig. S1). The major observations of this study are the following: (1) in line with our previous studies [20] atorvastatin was found to affect the proteomic profile of the EDL muscle more deeply than fluvastatin, likely due to its structural or pharmacokinetic characteristics; (2) atorvastatin mainly impaired the metabolic pathways responsible for energy production and particularly the key enzymes of the mitochondria, while fenofibrate essentially affected the glycolytic metabolism. Such a perturbation in energy metabolism and ATP synthesis may have

a profound impact on protein synthesis and cell viability [63]; (3) considering the pivotal role attributed to oxidative stress in many myopathies, the impairment of detoxification systems could play a major role in the development of myopathy; (4) since an impaired glycolytic metabolism was observed without alteration of MHC expression, the effects of statin and fenofibrate are independent of phenotype-specific gene reprogramming. This work adds important novel information regarding the molecular and functional mechanism of drug-induced muscle damage and opens the way to the discovery of new drug targets to counteract muscle toxicity.

Conflicts of interest

The authors declare no conflicts of interest.

Acknowledgements

Appendix A. Supplementary data

Supplementary data associated with this article can be found, in the online version, at doi:10.1016/j.bcp.2011.01.022.

References

[1] Goldstein JL, Brown MS. Regulation of the mevalonate pathway. Nature 1990;343:425–30.
[2] Cannon CP. Combination therapy in the management of mixed dyslipidaemia. J Intern Med 2008;263:353–5.
[3] Bellosta S, Paoletti R, Corsini A. Safety of statins: focus on clinical pharmacokinetics and drug interactions. Circulation 2004;109(23 (Suppl. 1)):III50–7.
[4] Rosenson RS. Statins: can the new generation make an impression? Expert Opin Emerg Drugs 2004;9(2):269–1269.
[5] Antons KA, Williams CD, Baker SK, Phillips PS. Clinical perspectives of statin-induced rhabdomyolysis. Am J Med 2006;119(5):400–9.
[6] Graham DJ, Staffa JA, Shatin D, Andrade SE, Schech SD, La Grenade L, et al. Incidence of hospitalized rhabdomyolysis in patients treated with lipid-lowering drugs. JAMA 2004;292(21):2585–90.
[7] Farmer JA. Learning from the cerivastatin experience. Lancet 2001;358(9291):1383–5.
[8] Gaist D, Rodríguez LA, Huerta C, Hallas J, Sindrup SH. Lipid-lowering drugs and risk of myopathy: a population-based follow-up study. Epidemiology 2001;12(5):565–9.
[9] Thompson PD, Clarkson P, Karas RH. Statin-associated myopathy. JAMA 2003;289(13):1681–90.
[10] Martin G, Duez H, Blanquart C, Berezowski V, Poulain P, Fruchart JC, et al. Statin-induced inhibition of the Rho-signaling pathway activates PPARalpha and induces HDL apoA-I. J Clin Invest 2001;107(11):1423–32.
[11] Weitz-Schmidt G. Statins as anti-inflammatory agents. Trends Pharmacol Sci 2002;23(10):482–6.
[12] Demierre MF, Higgins PD, Gruber SB, Hawk E, Lippman SM. Statins and cancer prevention. Nat Rev Cancer 2005;5(12):930–42.
[13] Evans M, Rees A. The myotoxicity of statins. Curr Opin Lipidol 2002;13(4):415–20.
[14] Vaughan CJ, Gotto Jr AM. Update on statins: 2003. Circulation 2004;110(7):886–92.
[15] Cornwell PD, De Souza AT, Ulrich RG. Profiling of hepatic gene expression in rats treated with fibric acid analogs. Mutat Res 2004;549(1–2):131–45.
[16] Mohaupt MG, Karas RH, Babiychuk EB, Sanchez-Freire V, Monastyrskaya K, Iyer L, et al. Association between statin-associated myopathy and skeletal muscle damage. CMAJ 2009;181(1–2):E11–18.
[17] Liantonio A, Giannuzzi V, Cippone V, Camerino GM, Pierno S, Camerino DC. Fluvastatin and atorvastatin affect calcium homeostasis of rat skeletal muscle fibers in vivo and in vitro by impairing the sarcoplasmic reticulum/mitochondria Ca2+-release system. J Pharmacol Exp Ther 2007;321(2):626–34.
[18] Pierno S, De Luca A, Liantonio A, Camerino C, Conte Camerino D. Effects of HMG-CoA reductase inhibitors on excitation-contraction coupling of rat skeletal muscle. Eur J Pharmacol 1999;364(1):43–8.
[19] Sirvent P, Mercier J, Vassort G, Lacampagne A. Simvastatin triggers mitochondria-induced Ca2+ signaling alteration in skeletal muscle. Biochem Biophys Res Commun 2005;329(3):1067–75.
[20] Pierno S, Camerino GM, Cippone V, Rolland JF, Desaphy JF, De Luca A, et al. Statins and fenofibrate affect skeletal muscle chloride conductance in rats by differently impairing ClC-1 channel regulation and expression. Br J Pharmacol 2009;156(8):1206–15.
[21] De Luca A, Tricarico D, Pierno S, Conte Camerino D. Aging and chloride channel regulation in rat fast-twitch muscle fibres. Pflugers Arch 1994;427(1–2):80–5.
[22] Bryant SH, Conte Camerino D. Chloride channel regulation in the skeletal muscle of normal and myotonic goats. Pflugers Arch 1991;417(6):605–10.
[23] Pierno S, De Luca A, Tricarico D, Roselli A, Natuzzi F, Ferrannini E, et al. Potential risk of myopathy by HMG-CoA reductase inhibitors: a comparison of pravastatin and simvastatin effects on membrane electrical properties of rat skeletal muscle fibers. J Pharmacol Exp Ther 1995;275(3):1490–6.
[24] Pierno S, Didonna MP, Cippone V, De Luca A, Pisoni M, Frigeri A, et al. Effects of chronic treatment with statins and fenofibrate on rat skeletal muscle: a biochemical, histological and electrophysiological study. Br J Pharmacol 2006;149(7):909–19.
[25] Pierno S, Desaphy JF, Liantonio A, De Luca A, Zarrilli A, Mastrofrancesco L, et al. Disuse of rat muscle in vivo reduces protein kinase C activity controlling the sarcolemma chloride conductance. J Physiol 2007;584(Pt 3):983–95.
[26] Spangenburg EE, Booth FW. Molecular regulation of individual skeletal muscle fibre types. Acta Physiol Scand 2003;178:413–24.
[27] Gelfi C, Vigano A, Ripamonti M, Pontoglio A, Begum S, Pellegrino MA, et al. The human muscle proteome in aging. J Proteome Res 2006;5(6):1344–53.
[28] Brocca L, D'Antona G, Bachi A, Pellegrino MA. Amino acid supplements improve native antioxidant enzyme expression in the skeletal muscle of diabetic mice. Am J Cardiol 2008;101(11A):57E–62E.
[29] Brocca L, Pellegrino MA, Desaphy JF, Pierno S, Camerino DC, Bottinelli R. Is oxidative stress a cause or consequence of disuse muscle atrophy in mice? A proteomic approach in hindlimb-unloaded mice. Exp Physiol 2010;95(2):331–50.
[30] Moriggi M, Vasso M, Fania C, Capitanio D, Bonifacio G, Salanova M, et al. Long term bed rest with and without vibration exercise countermeasures: effects on human muscle protein dysregulation. Proteomics 2010;10(21):3756–74.
[31] Steiner S, Gatlin CL, Lennon JJ, McGrath AM, Aponte AM, Makusky AJ, et al. Proteomics to display lovastatin-induced protein and pathway regulation in rat liver. Electrophoresis 2000;21(11):2129–37.
[32] Steiner S, Gatlin CL, Lennon JJ, McGrath AM, Seonarain MD, Makusky AJ, et al. Cholesterol biosynthesis regulation and protein changes in rat liver following treatment with fluvastatin. Toxicol Lett 2001;120(1–3):369–77.
[33] Kromer A, Moosmann B. Statin-induced liver injury involves cross-talk between cholesterol and selenoprotein biosynthetic pathways. Mol Pharmacol 2009;75(6):1421–9.
[34] Westwood FR, Scott RC, Marsden AM, Bigley A, Randall K, Rosuvastatin:. characterization of induced myopathy in the rat. Toxicol Pathol 2008;36(2):345–52.
[35] De Souza AT, Cornwell PD, Dai X, Caguyong MJ, Ulrich RG. Agonists of the peroxisome proliferator-activated receptor alpha induce a fiber-type-selective transcriptional response in rat skeletal muscle. Toxicol Sci 2006;92(2):578–86.
[36] O'Farrell PH. High resolution two-dimensional electrophoresis of proteins. J Biol Chem 1975;250(10):4007–21.
[37] Talmadge RJ, Roy RR. Electrophoretic separation of rat skeletal muscle myosin heavy-chain isoforms. J Appl Physiol 1993;75(5):2337–40.
[38] Pellegrino MA, Canepari M, Rossi R, D'Antona G, Reggiani C, Bottinelli R. Orthologous myosin isoforms and scaling of shortening velocity with body size in mouse, rat, rabbit and human muscles. J Physiol 2003;546(Pt 3):677–89.
[39] Laaksonen R, Katajamaa M, Päivä H, Sysi-Aho M, Saarinen L, Junni P, et al. A systems biology strategy reveals biological pathways and plasma biomarker candidates for potentially toxic statin-induced changes in muscle. PLoS ONE 2006;1(1):e97.
[40] Desaphy JF, Pierno S, Liantonio A, Giannuzzi V, Digennaro C, Dinardo MM, et al. Antioxidant treatment of hindlimb-unloaded mouse counteracts fiber type transition but not atrophy of disused muscles. Pharmacol Res 2010;61(6):553–63.
[41] Nemeth P, Pette D. Succinate dehydrogenase activity in fibres classified by myosin ATPase in three hind limb muscles of rat. J Physiol 1981;320:73–80.
[42] Schiaffino S, Reggiani C. Molecular diversity of myofibrillar proteins: gene regulation and functional significance. Physiol Rev 1996;76(2):371–423.
[43] Flück M, Hoppeler H. Molecular basis of skeletal muscle plasticity–from gene to form and function. Rev Physiol Biochem Pharmacol 2003;146:159–216.
[44] Päivä H, Thelen KM, Van Coster R, Smet J, De Paepe B, Mattila KM, et al. High-dose statins and skeletal muscle metabolism in humans: a randomized, controlled trial. Clin Pharmacol Ther 2005;78(1):60–8.
[45] Nakahara K, Kuriyama M, Sonoda Y, Yoshidome H, Nakagawa H, Fujiyama J, et al. Myopathy induced by HMG-CoA reductase inhibitors in rabbits: a pathological, electrophysiological, and biochemical study. Toxicol Appl Pharmacol 1998;152(1):99–106.
[46] Vaklavas C, Chatzizisis YS, Ziakas A, Zamboulis C, Giannoglou GD. Molecular basis of statin-associated myopathy. Atherosclerosis 2008;202(1):18–28.
[47] Nakagawa H, Mutoh T, Kumano T, Kuriyama M. HMG-CoA reductase inhibitor-induced L6 myoblast cell death: involvement of the phosphatidylinositol 3-kinase pathway. FEBS Lett 1998;438(3):289–92.
[48] Nishimoto T, Tozawa R, Amano Y, Wada T, Imura Y, Sugiyama Y. Comparing myotoxic effects of squalene synthase inhibitor, T-91485, and 3-hydroxy-3-methylglutaryl coenzyme A (HMG-CoA) reductase inhibitors in human myocytes. Biochem Pharmacol 2003;66(11):2133–9.

[49] Wang W, Wong CW. Statins enhance peroxisome proliferator-activated receptor gamma coactivator-1 alpha activity to regulate energy metabolism. J Mol Med 2010;88:309–17.

[50] Hanai J, Cao P, Tanksale P, Imamura S, Koshimizu E, Zhao J, et al. The muscle-specific ubiquitin ligase atrogin-1/MAFbx mediates statin-induced muscle toxicity. J Clin Invest 2007;117(12):3940–51.

[51] DiMauro S, Lamperti C. Muscle glycogenoses. Muscle Nerve 2001;24(8):984–99.

[52] Toscano A, Musumeci O. Tarui disease and distal glycogenoses: clinical and genetic update. Acta Myol 2007;26(2):105–7.

[53] Schaefer WH, Lawrence JW, Loughlin AF, Stoffregen DA, Mixson LA, Dean DC, et al. Evaluation of ubiquinone concentration and mitochondrial function relative to cerivastatin-induced skeletal myopathy in rats. Toxicol Appl Pharmacol 2004;194(1):10–23.

[54] Momken I, Lechene P, Koulmann N, Fortin D, Mateo P, Doan BT, et al. Impaired voluntary running capacity of creatine kinase-deficient mice. J Physiol 2005;565:951–64.

[55] Cabiscol E, Levine RL. Carbonic anhydrase III. Oxidative modification in vivo and loss of phosphatase activity during aging. J Biol Chem 1995;270(24):14742–7.

[56] Räisänen SR, Lehenkari P, Tasanen M, Rahkila P, Härkönen PL, Väänänen HK. Carbonic anhydrase III protects cells from hydrogen peroxide-induced apoptosis. FASEB J 1999;13(3):513–22.

[57] Tartakover-Matalon S, Cherepnin N, Kuchuk M, Drucker L, Kenis I, Fishman A, et al. Impaired migration of trophoblast cells caused by simvastatin is associated with decreased membrane IGF-I receptor, MMP2 activity and HSP27 expression. Hum Reprod 2007;22(4):1161–7.

[58] Schmeer C, Gámez A, Tausch S, Witte OW, Isenmann S. Statins modulate heat shock protein expression and enhance retinal ganglion cell survival after transient retinal ischemia/reperfusion in vivo. Invest Ophthalmol Vis Sci 2008;49(11):4971–81.

[59] Moylan JS, Reid MB. Oxidative stress, chronic disease, and muscle wasting. Muscle Nerve 2007;35:411–29.

[60] Powers SK, Kavazis AN, McClung JM. Oxidative stress and disuse muscle atrophy. J Appl Physiol 2007;102:2389–97.

[61] Hachiya N, Komiya T, Alam R, Iwahashi J, Sakaguchi M, Omura T, et al. MSF, a novel cytoplasmic chaperone which functions in precursor targeting to mitochondria. EMBO J 1994;13(21):5146–54.

[62] Ha CE, Ha JS, Theriault AG, Bhagavan NV. Effects of statins on the secretion of human serum albumin in cultured HepG2 cells. J Biomed Sci 2009;16: 16–32.

[63] Klawitter J, Shokati T, Moll V, Christians U, Klawitter J. Effects of lovastatin on breast cancer cells: a proteo-metabonomic study. Breast Cancer Res 2010;12(2):R16.